Journal of the Geological Society, London, Vol. **159**, 2002, pp. 751–761. Printed in Great Britain.

Attempted break-up of Rodinia at 850 Ma: geochronological evidence from the Seve–Kalak Superterrane, Scandinavian Caledonides

OSKAR PAULSSON & PER-GUNNAR ANDRÉASSON

Department of Mineralogy and Petrology, Lund University, Sölvegatan 13, S-223 62 Lund, Sweden
(e-mail: oskar.paulsson@geol.lu.se)

Abstract: Lower thrust sheets of the Scandinavian Caledonides derive from the margin of Baltica, which was imbricated during Early Palaeozoic closure of oceans formed during separation of the Baltica, Laurentia and Siberia cratons. At Vistas (Kebnekaise Mts), the Seve Nappe Complex preserves rare lenses of a dolerite-intruded granite formed by anatexis during emplacement of gabbro into metasedimentary rocks. Ion microprobe U–Pb dating of prismatic zircons from the granite yielded an age of 845 ± 14 Ma (mean square weighed deviation (MSWD) 1.15), interpreted to date magmatic crystallization. Cores of complex crystals indicate protolith ages of 1778 ± 11 Ma (MSWD 0.86); one core yielded an Archaean age. From narrow rims, a 605 ± 42 Ma metamorphic age is obtained, and is interpreted to reflect the emplacement of the extensive Vendian rift magmatic dolerite dyke swarm. The age pattern allows correlation with a previously dated magmatic complex within the equivalent Kalak Nappe Complex 300 km to the north. Bimodal magmatic complexes with this age pattern do not occur within the basement of the Caledonide foreland, nor elsewhere within the Baltic Shield. However, recent reinterpretations of the Knoydartian event in Scotland as rift related invites correlation with the West Highland Granite Gneiss, which intruded Moine metasedimentary rocks at *c*. 870 Ma. In Central Taimyr, 850–900 Ma granites of continental crustal derivation and with 1800–1900 Ma Sm–Nd model age occur associated with *c*. 740 Ma plagiogranites. Using recent palaeogeographical reconstructions, we interpret the evidence of 850–900 Ma magmatism in Scandinavia, Scotland and Taimyr as bimodal rift magmatism in connected arms during an attempted break-up of Rodinia.

Keywords: Scandinavia, Caledonides, Neoproterozoic, Rodinia, rifting, ion probe.

The Scandinavian Caledonides are a stack of thrust sheets emplaced onto the margin of Baltica during closure of early Phanerozoic North Atlantic oceans. Thrust sheets of lower tectonostratigraphic levels derive from the volcanic rifted margin of Baltica (Baltoscandian margin) formed during Neoproterozoic continental break-up. Thus, deformed and metamorphosed sedimentary and igneous rocks of the rift basins and their Precambrian basement plinths are preserved in the Seve and Kalak Nappe Complexes (for review, see Andréasson 1994). Recent palaeogeographical reconstructions of the Neoproterozoic North Atlantic tract relate formation of the Baltoscandian margin to the fragmentation of the supercontinent Rodinia into Baltica, Laurentia and Siberia (Torsvik *et al*. 1996; Dalziel 1997). In this study, new U–Pb data are reported on a Neoproterozoic granite body within the Seve Nappe Complex. Studies of Proterozoic rocks of this complex are useful for correlation and restoration of Caledonian allochthons to their precollisional locations, and for understanding the configuration of Proterozoic orogenic belts. Thus comparison is made with coeval magmatism in the Moine of the Scottish Highlands and with the Central Taimyr Complex of Siberia. The objective is to constrain available models of the Neoproterozoic palaeogeography in the present North Atlantic tract, with focus on Rodinia break-up.

Geological setting

The Neoproterozoic geological record of western Scandinavia reflects a setting of a volcanic rifted margin, referred to as the Baltoscandian margin (Gee 1975). Deposition in rift basins began at *c*. 800 Ma (Vidal & Nystuen 1990; Vidal & Moczydlowska 1995). During two major collision events (see Andréasson *et al*. (1998) and Grenne *et al*. (1999) for review) the Baltoscandian margin was subducted and imbricated, resulting in thrust sheets derived from the rift basins and their basement plinths. These thrust nappes now belong to the units referred to as the Paraautochthon and Lower, Middle and Upper Allochthons on tectonostratigraphic maps of the Scandinavian Caledonides (Figs. 1 and 2). Basement components of the nappes derive from belts truncated by the Caledonide belt (Fig. 1) including the Sveconorwegian (Grenvillian) belt (1.2–0.9 Ga); the Transscandinavian Igneous Belt (1.81–1.65 Ga); the 1.91–1.85 Ga Svecofennian belts and Karelian province, and the Archaean belts. Rocks of the allochthonous rift basins derive from Late Riphean to Vendian sedimentary cover successions, including Varangerian tillites, and are cut by extensive mafic dyke swarms (Kumpulainen & Nystuen 1985; Andréasson 1994). Andréasson *et al*. (1998) grouped all nappes characterized by Baltoscandian rift basin infill and rift magmatism into the Seve–Kalak Superterrane, a usage followed in this paper. One dolerite dyke swarm occurs *in situ* at Egersund in southernmost Norway, cutting the Sveconorwegian–Grenvillian basement of the Baltic shield. This swarm has been dated to 616 ± 3 Ma (U–Pb, baddeleyite; Bingen *et al*. 1998) in good agreement with an age of 608 ± 1 Ma (U–Pb zircon; Svenningsen 2001) obtained from the allochthonous sheeted dyke swarm in the Seve Nappe Complex (Sarek Mts).

Seve–Kalak Superterrane

The lowermost terranes, the Särv Nappes, are characterized by dolerites cutting alluvial to shallow marine sandstone sequences and their Precambrian basement. Subordinate rocks include thin

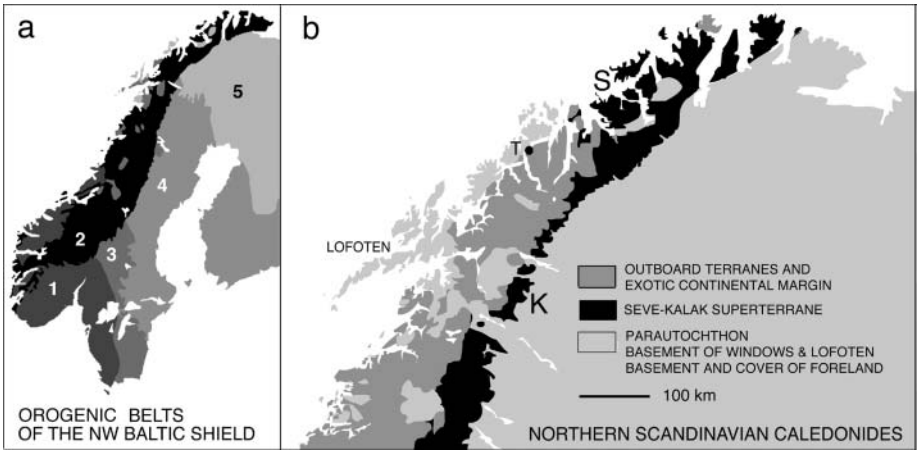

Fig. 1. Orogenic belts of the Baltic Shield in Scandinavia and principal terranes of the northern Scandinavian Caledonides. (**a**) 1, Sveconorwegian–Grenvillan belt; 2, Caledonide belt; 3, Transscandinavian Igneous Belt; 4, Svecofennian belts; 5, Karelian province and Archaean belts (**b**) K, Kebnekaise Mts (area of the Vistas Granite); S, Sørøy–Seiland area; T, Tromsø.

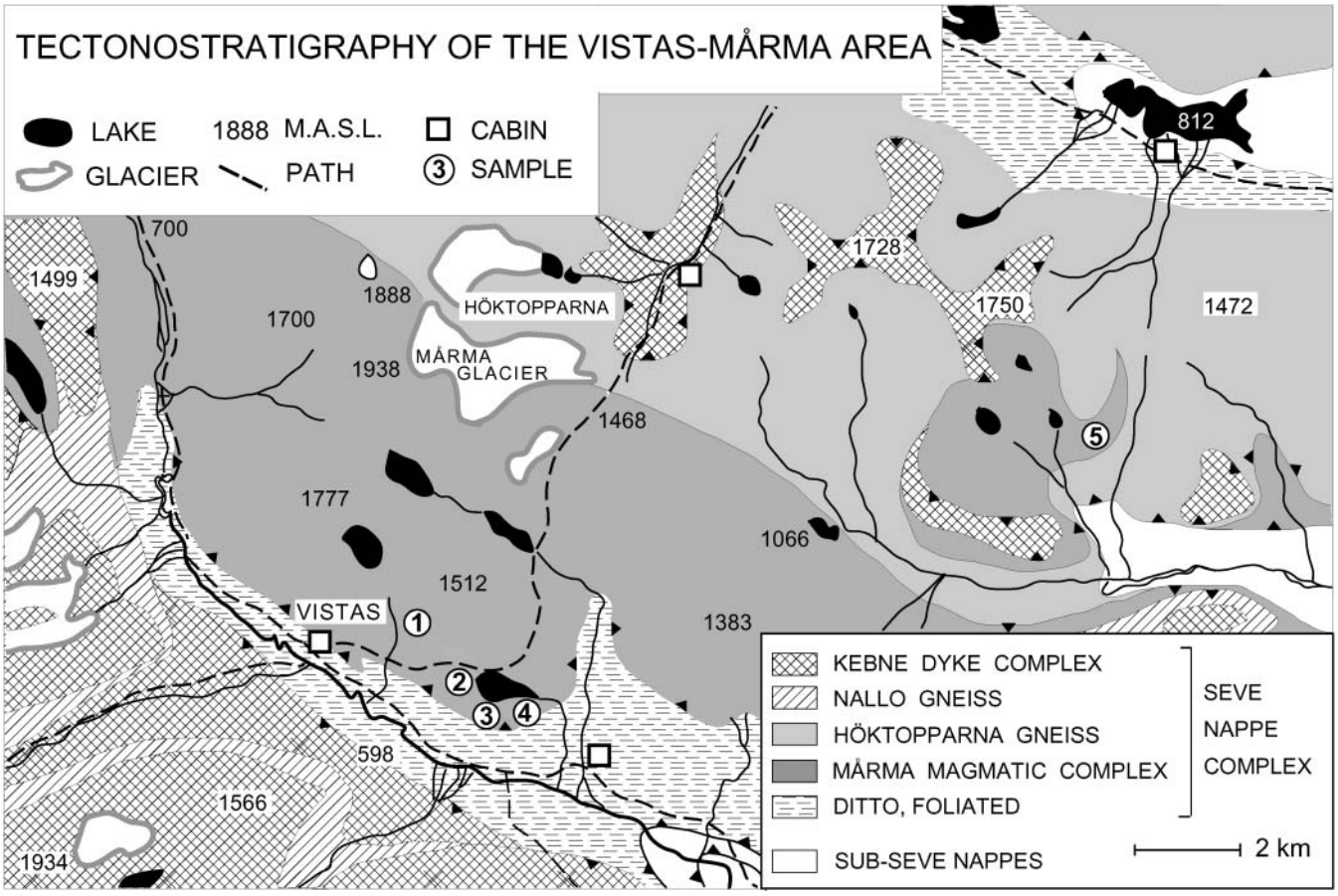

Fig. 2. Tectonostratigraphy of the Seve Nappe Complex in the Vistas area. Sample localities (Swedish National Grid): 1, sample K9353 [161916E, 755199N]; 2, sample VISTAS [161958E, 755039N]; 3, sample K9350 [161975E, 755050N]; 4, sample SM067B [162035E, 755039N]; 5, sample K9523 [163164E, 755567N].

units of dolomite, evaporite, Varangerian tillite and Precambrian crystalline rocks. When deformed and metamorphosed, rocks of the Särv Nappes are difficult to distinguish from the overlying basal nappe of the Seve Nappe Complex. The latter complex extends for 900 km northwards along the Swedish Caledonides. It includes metamorphosed lithologies derived from rift basins, from the outermost continental margin and from the ocean floor, i.e. psammitic and pelitic schists, orthogneisses, quartzites, marbles, meta-evaporites, calc-silicate gneisses, graphitic schists, mafic-dyke complexes, sheeted dyke complexes, amphibolites and ultramafites (Andréasson 1994; Andréasson *et al*. 1998). The Seve Nappe Complex exhibits very strong variation with regard to deformation and metamorphism, including pristine dolerite dykes cutting cross-bedded sandstones as well as eclogite boudins hosted in mylonitic or migmatitic gneisses (Andréasson *et al*. 1985).

Near the northern tip of Sweden, the Seve Nappe Complex passes into thick mylonites occurring between schists of the overlying Köli Nappes of oceanic derivation and psammites of the underlying Middle Allochthon (Stølen 1996). Farther north, in Finnmark, the Seve tectonostratigraphic level is occupied by the extensive Kalak Nappe Complex, composed of psammitic–pelitic cover above a Precambrian basement plinth (Ramsay *et al*. 1985). In the Seiland skerries, a large magmatic complex, the Seiland Igneous Province, occurs. It consists of gabbroic, ultramafic and alkaline rocks, mafic dyke swarms and carbonatites (Robins & Gardner 1975). These igneous rocks are hosted by metasedimentary rocks of the Sørøy Nappe (uppermost Kalak Nappe Complex) ranging from fluvial and shallow marine sandstones to distal turbidites (Roberts 1973). Small intrusions of quartz monzonite occur associated with the gabbros (Sturt & Taylor 1971). Within the intrusions, more or less preserved mafic dykes are present (Rice *et al*. 1991).

Vistas Granite

Augen gneisses and mylonitic gneisses abound in the Seve Nappe Complex of the Kebnekaise Mts. However, near Vistas, one type of augen gneiss grades into a comparatively massive granite (Vistas Granite), cut by dolerite dykes (Figs. 2 and 3a). Southeast of the Mårma glacier (Swedish National Grid E162100, N755670), the Vistas Granite occurs in a complex intrusive network with gabbroic rocks (Mårma Magmatic Complex; Fig. 2). Evidence of both mingling and mixing between granite magma and gabbro magma can be observed. Intrusive features are normally obscured by mylonitization of the wall-rock (Höktopparna Mylonite Gneiss). However, rare xenoliths of sedimentary rocks occur in the granite. Evidence of contact metamorphism of the wall-rock includes andalusite porphyroblasts enclosed in a fabric related to Caledonian nappe emplacement.

The Vistas Granite is a grey, medium-grained biotite granite with K-feldspar phenocrysts of *c*. 2 cm size. Accessory minerals include zircon, magnetite and rare apatite. Titanite, garnet and zoisite are secondary in origin. Foliated varieties of the granite are markedly rich in garnet. Myrmekite grew on K-feldspar phenocrysts during development of the foliation, indicating metamorphic temperatures of 500–600 °C (Harlov & Wirth, 2000).

Five samples were analysed for major and trace elements and REE (Table 1). According to standard classification methods based on major element contents, the Vistas Granite is a granite with high SiO_2 and K_2O/Na_2O (average 1.5) but low CaO (average 1.3). In the R1–R2 diagram of De la Roche *et al*. (1980) it classifies as a monzogranite (Fig. 4a). It is peraluminous with CIPW normative corundum. Incompatible element concentration patterns show negative spikes for Sr, P and Ti, reflecting the evolved state of the granite. The agreement with the concentration pattern of the upper continental crust is good. The Vistas Granite has a fractionated REE pattern (Fig. 4b;

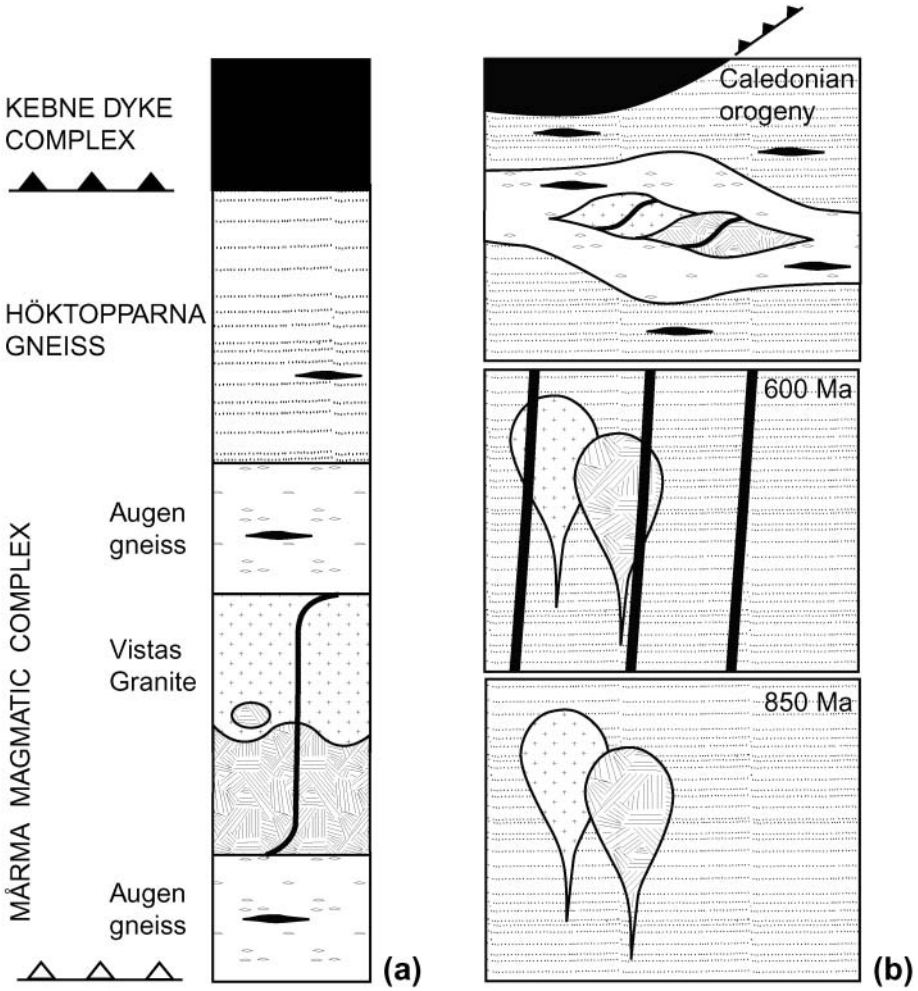

Fig. 3. (**a**) Tectonic stratigraphy of the Seve Nappe Complex in the Vistas area, Kebnekaise Mts. (**b**) Tectonic evolution of the Vistas area from 850 Ma to the Caledonian Orogeny suggested by results presented in this study.

Table 1. *Chemical whole-rock data for the Vistas Granite*

	K9350	K9353	K9523	SM067B	VISTAS
SiO_2	72.94	72.24	73.98	77.36	71.43
TiO_2	0.47	0.49	0.46	0.13	0.59
Al_2O_3	12.86	12.63	12.42	11.89	13.37
$Fe_2O_3{}^T$	3.29	4.17	3.19	1.44	3.8
MnO	0.06	0.09	0.05	0.05	0.06
MgO	0.57	0.37	0.4	0.17	0.7
CaO	1.2	1.21	1.19	0.58	1.57
Na_2O	2.87	3.19	2.85	3.19	3.2
K_2O	4.79	4.56	4.71	4.47	4.31
P_2O_5	0.12	0.09	0.05	0.05	0.13
Cr_2O_3	0.02	0.01	0.01	0.01	0.01
LOI	0.6	0.7	0.5	0.5	0.6
$CO_2{}^T$	0.01	0.01	0.01	0.01	0.01
$SO_2{}^T$	0.02	0.02	0.01	0.01	0.02
Sum	99.92	99.93	99.93	99.89	99.92
Ba	740	944	564	188	793
Bi	0.2	0.1	0.1	–	0.1
Co	44	33	43	40	37
Cs	3.8	5.3	2.7	4.9	2.1
Ga	21	24	21	19	21
Hf	9.1	17.2	11.1	4.5	11.4
Nb	12	20	8	7	15
Rb	198	189	227	260	152
Sn	3.4	5.7	6.0	4.1	1.2
Sr	139	114	82	45	155
Ta	0.7	1.2	0.5	0.7	0.6
Th	12	11	15	7	17
Tl	0.7	0.7	0.8	0.8	0.5
U	2.3	2.7	4.0	2.9	2.1
V	30	15	21	7	36
W	319	241	313	303	252
Zr	344	602	390	134	418
Y	59	93	47	41	44
La	38	28	25	15	59
Ce	87	65	55	35	118
Pr	9	8	7	4	14
Nd	43	33	30	18	64
Sm	9	9	7	5	12
Eu	1.4	1.6	1.3	0.5	1.6
Gd	7.7	9.0	6.6	4.4	10.8
Tb	1.5	2.1	1.2	1.0	1.7
Dy	9.2	13.4	7.2	6.0	8.0
Ho	2.0	3.4	1.7	1.4	1.7
Er	5.5	9.0	4.3	3.9	3.8
Tm	0.9	1.6	0.7	0.7	0.5
Yb	5.2	9.9	4.1	4.8	3.0
Lu	0.9	1.7	0.7	0.8	0.5

Major elements in wt %; trace element in ppm. (See text for analytical details.)

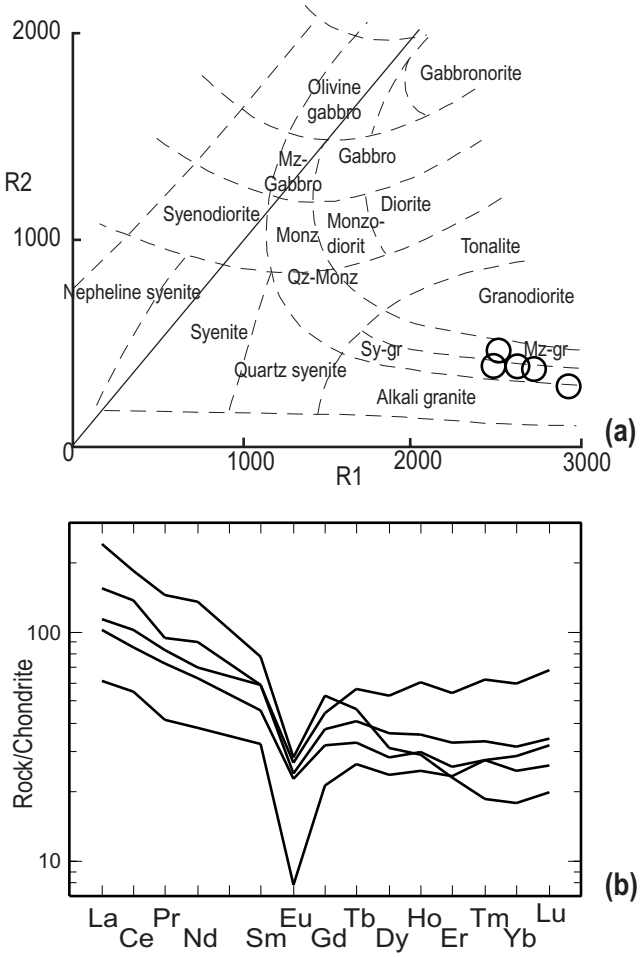

Fig. 4. (**a**) Classification of the Vistas Granite according to the R1–R2 method of De la Roche *et al*. (1980) based on five samples. (**b**) Chondrite-normalized REE patterns of five samples of the Vistas Granite. Normalizing values were taken from Evensen *et al*. (1978).

average La_N/Lu_N is 5.4) with slight enrichment in light REE (LREE; average La_N/Sm_N is 2.6). All analysed samples show distinct negative Eu anomalies. In summary, the Vistas Granite has a composition of S-type granite (Chappell & White 1992) and plots in the field of within-plate granites in Y–Nb and Y + Nb–Rb discrimination diagrams of Pearce *et al*. (1984).

The Vistas Granite was intruded by dolerites, which preserve chilled margins. On the basis of petrographic and chemical properties, Sandelin (1997) compared the dolerites with the mildly alkaline to transitional, *c*. 1220 Ma Central Scandinavian Dolerite Group of the Caledonian foreland (Solyom *et al*. 1992) or with the alkaline subgroup of Baltoscandian rift-facies dolerites occurring within the Särv nappes (see above; Solyom *et al*. 1984). As the present paper demonstrates that the Vistas Granite is younger than 1220 Ma, the former alternative can now be excluded.

Sampling and methods

Five samples were used for geochemical analysis and one of these samples was selected for ion microprobe analysis. Four of the samples were crushed using standard technique and then processed for 120 s in a tungsten-carbide grinder to produce powder for geochemical analysis. The fifth sample (VISTAS) was, after crushing, processed for 10 s in a tungsten-carbide grinder and then split into two fractions. One fraction was prepared on a Wilfley table for separation of minerals by density. From the most dense mineral separate garnets were removed by electromagnet, and zircons were then handpicked. The second fraction was processed for another 120 s in the tungsten-carbide grinder for whole-rock chemical analysis.

Ion microprobe technique

The handpicked zircons from the VISTAS sample were cast in epoxy and polished, leaving half crystals exposed. Zoning of the crystals was characterized using backscattered electron (BSE) imaging, and zircon domains suitable for ion microprobe analysis were selected using these images. Great care was taken to select homogeneous domains. The U–Th–Pb analysis was performed

at the Laboratory for Isotope Geology at the Museum of Natural History in Stockholm, using the CAMECA IMS 1270 ion microprobe of the NORDSIM laboratory. Analytical procedures closely followed those described by Whitehouse *et al*. (1997a, 1997b, 1999). The analysed domains are *c*. 30 μm in diameter and a less than a micron deep. The program ISOPLOT of Ludwig (1999) was used for all age calculations. The analyses were captured during three sessions. During the last session, Hf-carbide interfered with the ^{204}Pb analysis and no reliable ^{206}Pb/^{204}Pb ratio could be calculated from this session. The Hf-carbide was probably produced by a reaction between hafnium in the zircon and carbon left in cracks from the coating used for BSE imaging. The sample was recoated before the last session. Therefore, common Pb correction based on measured ^{204}Pb assuming present-day composition of terrestrial Pb (Stacey & Kramers 1975) was performed only on the data collected during the two first sessions. However, it is known that the ^{206}Pb/^{204}Pb ratio will be very high on ion microprobe analysis if, as in this study, only homogeneous areas with no inclusions are analysed. The correction according to Stacey & Kramers (1975) will accordingly often be very small and the effect of the Hf-carbide contamination on the results of this study is considered negligible. Nevertheless, data with Pb corrections are not used together with data without corrections in ISOPLOT for mean age calculations. The standard zircon used is Geostandard 91500 (Wiedenbeck *et al*. 1995). Analytical results from the individual spots are presented in Table 2 with 1σ error. Ages discussed in the text are given with 2σ errors.

Inductively coupled plasma mass spectrometry (ICP-MS)

In this study two types of ICP-MS analysis were performed. ICP-MS analysis on dissolved whole-rock samples for major and trace elements and REE was performed at the commercial ACME Analytical Laboratories Ltd. in Vancouver using $LiBO_2$ fusion. Laser ablation ICP-MS analysis for REE in zircons was performed at the Department of Earth Science, Gothenburg University, using an Hp4500 ICP quadrupole mass spectrometer connected with a Cetac LSX 200 UV-laser. The laser used 0.5 mJ per shot and had a wavelength of 266 nm. The laser beam was 50 μm in diameter and it had a frequency of 10 Hz. As external standard NIST 612 (Pearce *et al*. 1997) was used; silica was measured as an internal standard with a reference stoichiometric value of 49.5%.

Geochronological results

BSE images

Two populations of zircon occur in the Vistas Granite: one consists of stubby crystals and the other of elongate prisms (Fig. 5). Stubby crystals are complex, typically with two oscillatory zoned domains. Most of the crystals show a distinct and homogeneous rim characterized by dark contrast on BSE images (low average atomic weight; Fig. 5). The size varies from 100 to 200 μm and length/width ratios from one to two. Elongate

Table 2. *U–Th–Pb data obtained by ion microprobe (NORDSIM) analysis of zircons from the Vistas Granite*

Zircon[1]	Spot[2]	[U] (ppm)	[Th] (ppm)	[Pb] (ppm)	Th/U calc.[3]	^{207}Pb/^{206}Pb	± σ (%)	^{207}Pb/^{235}U	± σ (%)	^{206}Pb/^{238}U	± σ (%)	*r*	Disc (%)	^{206}Pb/^{204}Pb	^{207}Pb/^{206}Pb age (Ma)	± σ (Ma)	^{206}P/^{238}U age (Ma)	± σ (Ma)
1 s	1	90	34	34	0.35	0.1104	1.05	4.6461	3.67	0.3053	3.52	0.96		56630	1805	19	1718	53
2 s +	1 c	438	350	353	0.85	0.2057	0.43	15.6961	1.78	0.5536	1.73	0.97		34060	2872	7	2840	40
2 s	2 r	171	31	41	0.18	0.0931	0.82	1.9845	1.8	0.1546	1.6	0.89	−39	18360	1490	16	927	14
2 s +	3 c	427	332	335	0.83	0.2026	0.24	15.1331	0.96	0.5418	0.93	0.97	−1	110230	2847	4	2791	21
3 s	1	65	25	16	0.25	0.1094	1.02	4.9618	1.71	0.3290	1.37	0.80	0	108240	1789	19	1834	22
4 s	1 r	57	11	31	0.69	0.0646	2.14	1.3860	2.93	0.1555	2.01	0.68	19	8530	762	45	932	17
4 s	2 c	437	102	204	0.55	0.0723	0.27	1.9077	0.78	0.1915	0.73	0.94	13	108580	993	6	1129	8
5 s +	1 r	109	11	4	0.03	0.0600	0.97	0.7802	1.46	0.0943	1.1	0.75		9050	605	21	581	6
6 s	1 c	65	41	10	0.54	0.0682	1.32	1.1134	1.74	0.1184	1.14	0.66	−9	12995	876	27	722	8
7 s	1 c	240	83	66	0.30	0.0913	0.60	2.9103	1.06	0.2312	0.87	0.82	−4	78431	1446	11	1341	11
7 s	2 r	308	32	40	0.09	0.0672	0.73	1.0792	1.13	0.1165	0.86	0.76	−12	58582	846	15	710	6
5 s	2 c	128	57	42	0.38	0.1117	0.68	4.0478	1.15	0.2628	0.93	0.81	−15	>1e6	1815	12	1504	13
8 s	1 c	166	39	45	0.19	0.1046	0.70	3.3515	1.71	0.2324	1.56	0.91	−18	12962	1697	13	1347	19
8 s	2 c	295	98	90	0.29	0.1020	0.97	3.5797	1.64	0.2544	1.32	0.81	−7	50736	1652	18	1461	17
8 s	3 r	123	40	19	0.30	0.0665	1.90	1.2524	2.23	0.1367	1.17	0.53		4355	823	39	826	9
9 s	1	549	86	151	0.12	0.1055	0.38	3.4801	0.94	0.2392	0.86	0.91	−19	103242	1712	7	1383	11
10 s	1	88	45	25	0.42	0.0990	1.93	3.0690	2.12	0.2248	0.89	0.42	−10	32927	1597	35	1307	11
11 s	1	156	85	48	0.46	0.1113	0.65	3.6246	1.07	0.2362	0.85	0.79	−23	>1e6	1808	12	1367	10
12 s +	1	229	146	92	0.57	0.1079	0.39	4.7407	1.06	0.3157	0.99	0.94		13545	1781	7	1769	15
13 e +	1	140	73	24	0.49	0.0636	1.24	1.2971	1.18	0.1385	0.89	0.75		3307	867	16	836	7
14 s	1	131	60	56	0.45	0.1133	0.46	5.4688	1.02	0.3473	0.92	0.91	1	15291	1867	8	1922	15
15 e +	1	273	18	42	0.07	0.0625	0.96	1.3070	1.07	0.1412	0.89	0.83		3125	842	13	851	7
16 e	1	366	115	59	0.25	0.0671	0.74	1.2790	1.04	0.1413	0.9	0.87	3	4810	796	11	852	7
17 e	1	202	55	–	–	0.0501	3.14	1.4307	1.15	0.1466	0.89	0.77	−3	710	952	15	882	7
18 e	1	224	56	37	0.23	0.0479	3.34	1.3201	1.24	0.1472	0.89	0.72	8	860	776	18	885	7
7 s	3 c	125	52	42	0.43	0.0924	0.57	3.5328	1.34	0.2760	1.22	0.91	3	31776	1485	11	1571	17
7 s +	4 r	342	47	55	0.15	0.0663	0.77	1.3233	1.16	0.1441	0.89	0.77		47529	826	15	868	7
19 e +	1	161	153	31	0.93	0.0665	1.06	1.3312	1.36	0.1442	0.9	0.66		34566	837	21	868	7
5 s +	3 c	177	99	71	0.53	0.1089	0.86	4.7514	1.23	0.3162	0.88	0.72		98814	1783	16	1771	14
20 s +	1 c	76	54	32	0.63	0.1075	0.65	4.7776	1.09	0.3211	0.89	0.81		34305	1764	12	1795	14
20 s	2 r	271	20	–	–	0.0578	3.28	1.2448	1.16	0.1287	0.96	0.83	−13	1176	933	13	780	7
6 s +	2 c	143	49	25	0.24	0.0668	1.44	1.4493	1.6	0.1545	0.97	0.61		11774	870	26	926	8
21 s	1	196	154	94	0.79	0.1101	0.44	5.5620	1	0.3657	0.9	0.9	10	59952	1804	8	2009	16

Disc. (%) refers to the degree of discordance of ^{207}Pb/^{206}Pb and ^{206}Pb/^{238}U ages at the 2σ error limit. All zircons are from sample VISTAS, sample location 2 in Fig. 2. Analyses in the upper part of the table were obtained during the two first sessions and corrected for common Pb according to Stacey & Kramers (1975) at 0 Ma. Analyses in the lower part of the table were obtained during the third session when no common Pb correction was made because of interference by Hf-carbide (see text).

[1]Zircon number and shape of the zircon (s, stubby; e, elongated); +, analysis used in the age calculation.

[2]Spot number and domain (c, core; r, rim).

[3]Th/U ratio calculated from measured ThO intensity.

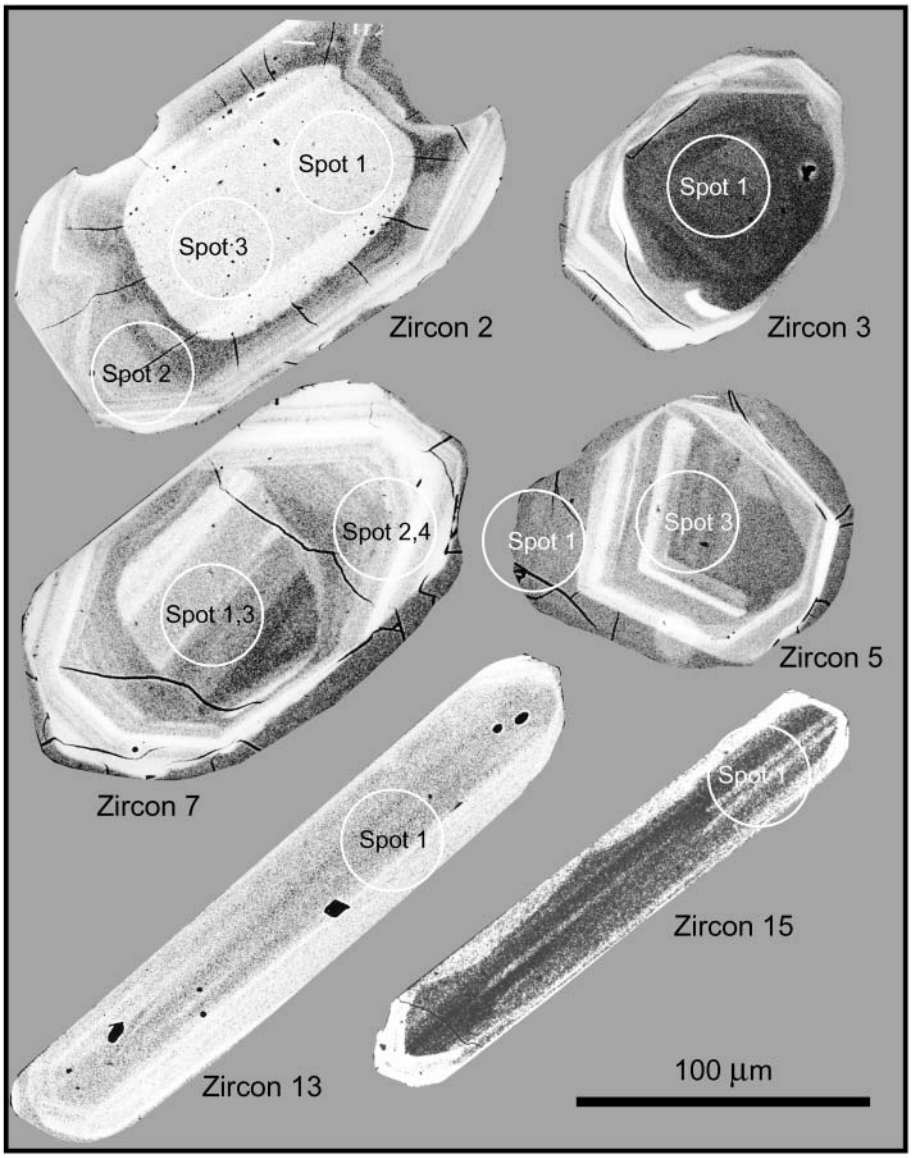

Fig. 5. Backscattered electron images of zircons of the Vistas Granite. White circles indicate analysed spots. Ages for the individual analyses with 1σ errors are as follows. Zircon 2: spot 1, 2872 ± 7 Ma; spot 2, 1490 ± 16 Ma; spot 3, 2847 ± 4 Ma. Zircon 3: spot 1, 1789 ± 19 Ma. Zircon 7: spot 3, 1485 ± 11 Ma; spot 4, 826 ± 15 Ma. Zircon 5: spot 1, 605 ± 21 Ma; spot 3, 1783 ± 16 Ma. Zircon 13: spot 1, 867 ± 16 Ma. Zircon 15: spot 1, 842 ± 13 Ma.

crystals are zoned but lack a complex internal structure with cores and rims, and are typically 200 µm long and 40 µm wide.

Ion microprobe results

From the analysed sample (VISTAS), a total of 33 spots were analysed in 21 zircons. Zircon growth in four time intervals was detected: Archaean, Palaeoproterozoic, Neoproterozoic and late Neoproterozoic (Fig. 5; Table 2). The Archaean and late Neoproterozoic ages are obtained from data corrected for common Pb whereas the Palaeoproterozoic and Neoproterozoic ages are obtained from uncorrected data. As corrected and uncorrected data are not combined, a few corrected analyses yielding Palaeoproterozoic and Neoproterozoic ages are excluded from the mean age calculations. Two spots (zircon 2, spots 1 and 3) from the core of a stubby zircon yield a $^{207}Pb/^{206}Pb$ weighted mean age of 2851 ± 130 Ma (mean square weighted deviation (MSWD) 9.5, 2σ error; Figs. 5 and 6a). From the rim of this Archaean core, a discordant $^{207}Pb/^{206}Pb$ age of 1490 Ma is obtained (spot 2). Twelve spots from 10 stubby zircons yield Palaeoproterozoic ages; seven of these are excluded from the age calculation because of discordance, two are excluded because these data are corrected for common Pb. The remaining three spots yield a $^{207}Pb/^{206}Pb$ weighted mean age of 1778 ± 11 Ma (MSWD 0.86; 2σ error; Fig. 6b). In Table 2 these spots include zircon 12 (spot 1), zircon 5 (spot 3) and zircon 20 (spot 1). From 11 crystals, both stubby and elongate, 14 spots yield Neoproterozoic ages. Eight spots are excluded from the mean age calculation because of discordance and one because it is corrected for common Pb. The remaining five analyses give a $^{207}Pb/^{206}Pb$ weighted mean age of 845 ± 14 Ma (MSWD 1.15, 2σ error; Fig. 6c). In Table 2 these analyses include zircon 13 (spot 1), zircon 15 (spot 1), zircon 7 (spot 4), zircon 19 (spot 1) and zircon 6 (spot 2). One dark thin rim, typically seen on stubby zircons, is thick enough to be analysed. A concordant $^{207}Pb/^{206}Pb$ age of 605 ± 42 Ma (2σ error) is obtained (zircon 5, spot 1; Figs. 5 and 6d). Two analyses with a $^{207}Pb/^{206}Pb$ age of 1446 Ma and 1485 Ma (zircon 7, spots 1 and 3) are obtained from the core of a stubby zircon (Fig. 5). The rim of this zircon gives an age of 826 Ma (spot 4). The Th/U ratio (average 0.42) suggests that all domains but the dark rim have a magmatic origin (Table 2). The dark rim has a ratio of 0.03, typical for zircon growth during metamorphism.

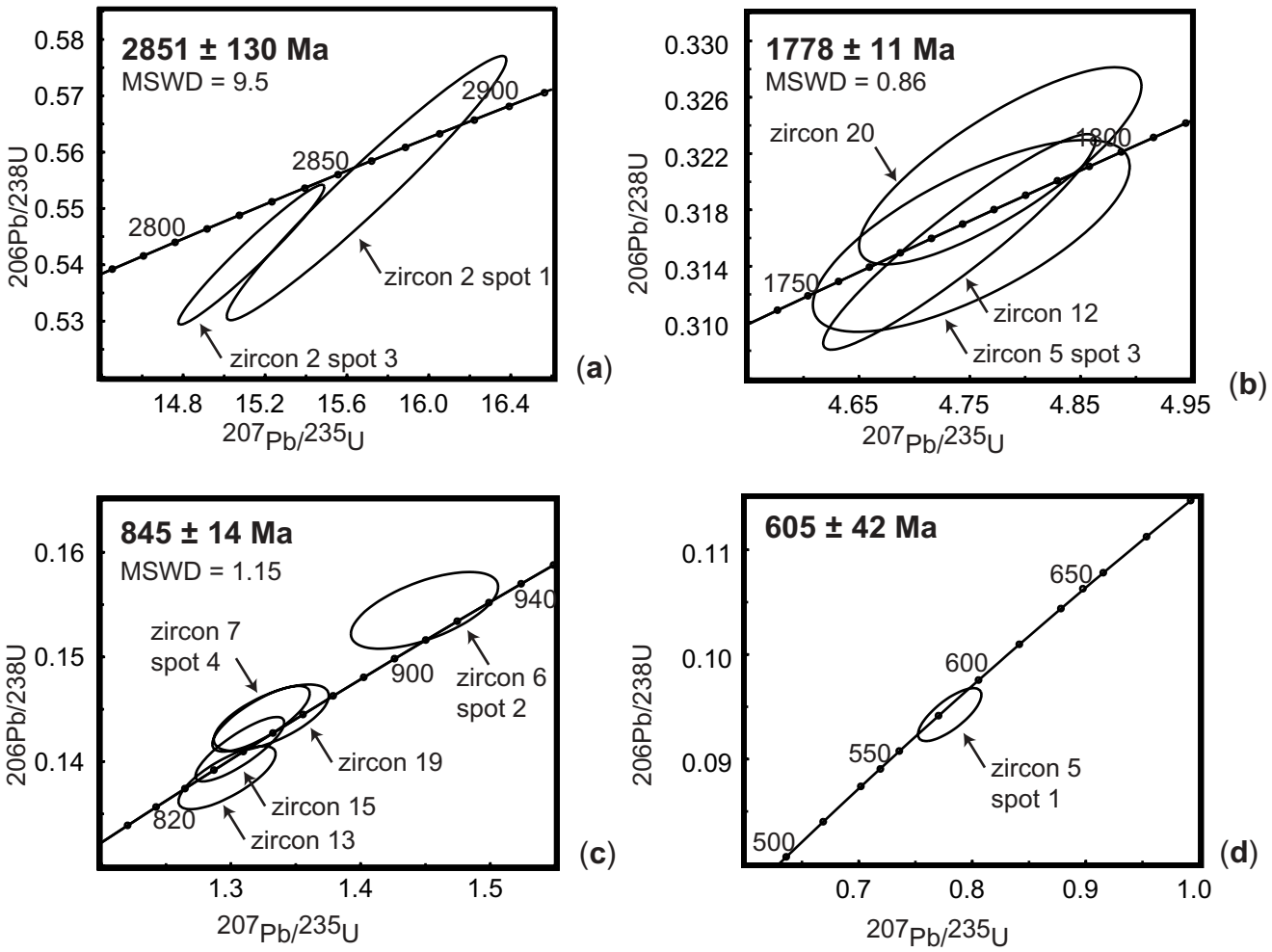

Fig. 6. U–Pb concordia diagram of data obtained by ion microprobe (NORDSIM) analysis of zircons from the Vistas Granite. Only analyses used in age calculations are shown; a complete record is found in Table 2. All ages are shown with 2σ errors. (**a**) Archaean age based on two analyses (zircon 2, spots 1 and 3). (**b**) Palaeoproterozoic age based on three analyses (zircon 12; zircon 5, spot 3; zircon 20 spot 2). (**c**) Neoproterozoic age based on five analyses (zircon 13; zircon 15; zircon 7, spot 4; zircon 19; zircon 6, spot 2). (**d**) Late Neoproterozoic age based on one analysis (zircon 5, spot 1).

Results of zircon REE analysis

The core and the rim of zircon 5 shown in Fig. 5 were analysed for REE with laser ablation ICP-MS. This is the only crystal exposing a dark rim thick enough for ion microprobe and laser ICP-MS analysis. The laser beam was aimed at the core (spots 2 and 3) and at the rim (spot 1). Both core and rim had been analysed earlier by ion probe, yielding ages of 1783 Ma and 605 Ma, respectively. Both domains show a marked enrichment in heavy REE (HREE) typical for zircon (Fig. 7; Table 3). The Yb/Gd ratio is seven for the core and 13 for the rim. The La concentration of the core is at or below the detection limit, resulting in an irregular pattern with a probable negative Eu anomaly and a positive Ce anomaly. In contrast, the rim has a rather smooth LREE pattern with minor negative anomalies in Eu and Ce.

Interpretation

Because of their shape, lack of cores and Th/U ratio (average 0.38), the elongate zircons are interpreted as magmatic crystals grown during crystallization of the Vistas Granite at 845 ± 14 Ma (Fig. 5, zircons 13 and 15). The discordant analysis giving an age of 1490 Ma obtained from the rim surrounding the Archaean core (Fig. 5, zircon 2) could result from mixed sampling of the two domains, i.e. the *c*. 845 Ma magmatic domain and the *c*. 2850 Ma core. From a core of a stubby zircon,

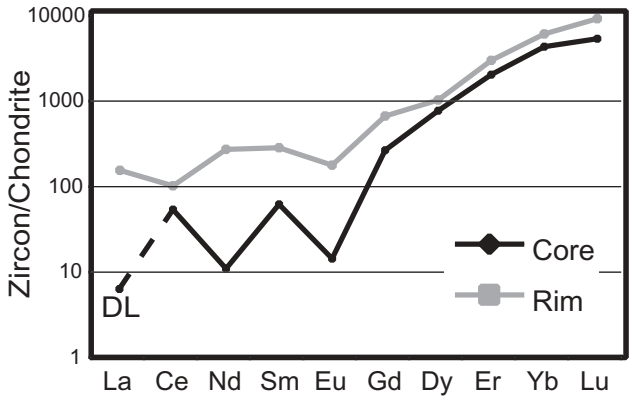

Fig. 7. Comparison of REE patterns of rim and core of zircon 5 shown in Fig. 4. DL, detection limit for La for the instrument used. Chondrite normalizing values from Evensen *et al*. (1978).

Table 3. *Rare earth element concentrations of zircon 5 shown in Fig. 4*

	Core (ppm)	Rim (ppm)
La	b.d.	35
Ce	32	61
Nd	5	121
Sm	9	41
Eu	1	10
Gd	51	128
Dy	184	244
Er	317	464
Yb	669	941
Lu	128	219

The zircon yielded an age of *c*. 1780 Ma and 605 Ma for the core and rim, respectively (zircon 5, spot 3 and spot 1; Table 2). b.d., concentration below detection limit.

two analyses (Fig. 5, zircon 7) resulted in ages of *c*. 1446 Ma and *c*. 1485 Ma, respectively. These analyses are not concordant, which makes interpretations ambiguous. The shape of the Archaean core suggests a detrital history.

We propose that the source of the Vistas Granite is a sedimentary rock with at least one Palaeoproterozoic (1778 Ma) and one Archaean (2850 Ma) component. After intrusion at 845 ± 14 Ma, the granite was intruded by a dense swarm of dolerite dykes. The rise in temperature following intrusion of the dike complex and the possibly associated mobilization of fluid in the mica-rich granite could have triggered growth of metamorphic zircon in the granite. The 605 ± 42 Ma dark metamorphic rims found on many zircons are interpreted to date the intrusion of the dyke swarm. The age is in good agreement with dated rift-facies dykes from the same nappe complex (Sarek, 608 ± 1 Ma) and the basement (Egersund, 616 ± 3 Ma; see 'Geological setting').

The zircon crystalline structure accommodates HREE more easily than LREE, because of the smaller ion radius of the HREE. Consequently, zircon generally displays an HREE-enriched pattern. However, Harley (2001) showed that if zircon coexists with garnet during crystallization, the HREE are preferentially partitioned into the garnet, resulting in flat HREE patterns of the zircons. The REE pattern obtained from the metamorphic rim of zircon 5 shows enrichment in HREE (Fig. 7), indicating that the garnets found in the granite grew during a different event, probably during Caledonian nappe emplacement. The REE patterns show also some difference between core and rim for the LREE. Normally magmatic zircons have steep LREE to HREE patterns, a strong positive Ce anomaly and a weak negative Eu anomaly (Whitehouse 2000). Despite the erratic pattern, the core shows these characteristics whereas the rim lacks the positive Ce anomaly. Thus the REE patterns obtained from the Vistas Granite suggest a magmatic origin for the core and a metamorphic origin for the rim, as indicated by the ion microprobe data.

Discussion and conclusions

Correlation within the Caledonide belt

Granitic bodies with composition, geological setting and age similar to the Vistas Granite have so far not been found in the Seve Nappe Complex, the Caledonide foreland of Scandinavia, or elsewhere in the Baltic Shield. However, the ion microprobe data allow correlation along the orogenic belt. In the uppermost Kalak Nappe Complex (Sørøy Nappe) at an equivalent tectonostratigraphic level, granitic dykes and gabbro intrusions of similar age occur in the Sørøy–Seiland area (Fig. 1b; Table 4) hosted in high-grade psammitic gneisses, migmatites and orthogneisses (Sturt & Taylor 1971; Roberts 1973; Robins & Gardner 1975; Krogh & Elvevold 1990; Daly *et al*. 1991; Rice *et al*. 1991; Reginiussen *et al*. 1995). The host rocks have striking lithological, metamorphic and structural similarities to those of the Vistas Granite in the Kebnekaise Mts (Höktopparna Gneiss). The dated granitic dykes (U–Pb zircon age of 804 ± 19 Ma; Daly *et al*. 1991) grade into augen gneisses. Gabbro and monzonite intrusions considered to have been emplaced during initial continental rifting (Reginiussen *et al*. 1995) yield an age of 829 ± 18 Ma (Rb–Sr whole-rock age; Krogh & Elvevold 1990). A second event of gabbro intrusion occurred at *c*. 700 Ma (Daly *et al*. 1991). At 600–550 Ma (Pedersen *et al*. 1989; Daly *et al*. 1991), a continental rift magmatic suite of gabbros, ultramafites, alka-

Table 4. *Comparison of radiometric age patterns of magmatic rocks obtained in the present study (Vistas) and reported from the Kalak Nappe Complex of the Sørøy–Seiland Province and from the Central Taimyr Belt*

Age, Seve Nappe Complex at Vistas (this study) (Ma)	Age, Kalak Nappe Complex at Sørøy–Seiland (Ma)	Methods	Age, Central Taimyr Belt (Ma)	Methods
605 ± 42 Thermal metamorphism			626–575 Regional metamorphism	Sm–Nd, Rb–Sr, Ar–Ar, K–Ar (1)
	700 ± 33 Gabbro intrusion	Rb–Sr (2)	720–740 Plagiogranite	U–Pb zircon (1)
845 ± 14 Granite intrusion	804 ± 19 Granite intrusion	U–Pb (2)	785–850 Model ages	Sm–Nd (1)
	829 ± 18 Gabbro intrusion	Rb–Sr (3)	885 ± 11–894 ± 15 923 ± 11; 940 ± 17 Granite intrusion	U–Pb zircon, ion probe (4, 5)
1778 ± 11 Inherited zircon	1730 ± 216 Granite intrusion, upper intercept 1200–1800 Model ages	U–Pb zircon (2) Sm–Nd (6)	1800–1900 Model ages 1800–2000 Model ages	Sm–Nd (1) Sm–Nd (4)
2851 ± 130	2800 Model ages	Sm–Nd (6)	2200–2600	U–Pb zircon xenocryst, ion probe (5)

References (numbers in parentheses): 1, Vernikovskiy *et al*. (1998); 2, Daly *et al*. (1991); 3, Krogh & Elvevold (1990); 4, Vernikovskaya *et al*. (2001); 5, Pease *et al*. (2001); 6, Aitcheson (1990).

line basaltic dykes and carbonatites was emplaced into the old gabbro–granite complex. The basement structurally underlying the Sørøy metasedimentary rocks includes Archaean orthogneiss or paragneiss. Aitcheson (1990) obtained Sm–Nd model ages of 2.8 Ga and 1.2–2.0 Ga from ortho- and paragneiss of the Kalak Nappe Complex. Thus the available geochronological results on magmatic suites substantiate a correlation between the units of the Seve Nappe Complex treated here (Mårma Magmatic Complex; Höktopparna Gneiss) and the Sørøy Nappe of the Kalak Nappe Complex.

Correlation within the Neoproterozoic North Atlantic tract

Scottish Highlands. Daly *et al*. (1991) referred to the pre-800 Ma event of deformation and metamorphism of the Kalak Nappe Complex as the Porsanger Orogeny and discussed a correlation with the Scottish Highlands based on the evidence of a Morarian (Knoydartian; 750–815 Ma) tectonometamorphic event. Recent geochronological work including a high-precision U–Pb technique has confirmed pegmatite generation and tectonometamorphism between 750 and 840 Ma (Noble *et al*. 1996; Rogers *et al*. 1998). Of particular interest to this study is the upper intercept zircon age of 873 ± 7 Ma for the Ardgour granite gneiss (Friend *et al*. 1997). The Ardgour granite gneiss is one of the deformed and metamorphosed granites intruding sedimentary rocks of the Moine Supergroup and collectively referred to as the West Highland Granite Gneiss. Magmatic zircon needles yield a weighted average age of 870 ± 48 Ma (ion microprobe data) and detrital zircons a range of inherited ages from 1100 to 1900 Ma. The protolith of the West Highland Granite Gneiss is described as S-type, anatectic granite derived from partial melting of sedimentary rocks of the Moine Supergroup. Mafic intrusions in the sedimentary rocks include dolerites of MORB affinity and gabbro, both rock types now amphibolitized and occurring as sheets (Winchester 1985; Millar 1999). Millar (1999) obtained a U–Pb zircon age of 873 ± 6 Ma for the metagabbro; that is, an age identical to that of the Ardgour granite gneiss.

Central Taimyr. In the Neoproterozoic Central Taimyr Belt of Arctic Siberia, granites with similar age patterns (*c*. 600 Ma; *c*. 740 Ma; 785–850 Ma; 880–940 Ma; see Table 4) occur in the Mamont–Shrenk Terrane (Vernikovskiy *et al*. 1998; Pease *et al*. 2001; Vernikovskaya *et al*. 2001; Vernikovsky & Vernikovskaya 2001, and references therein). An associated *c*. 740 Ma complex of ultramafic and gabbroic rocks, and dolerites of N-MORB to E-MORB affinities has been referred to as ophiolites and interpreted to be related to the initial break-up of Rodinia (Vernikovsky & Vernikovskaya 2001). Plagiogranites of this ophiolite complex yield an age of 720–740 Ma. The Mamont–Shrenk Terrane and the ophiolite amalgamated and accreted to the Siberian craton before late Vendian time (Pease *et al*. 2001). Cover rocks of Late Vendian to Early Carboniferous age overlap the accreted complex. S-type granites of the complex formed between 850 and 940 Ma from continental crust with Sm–Nd model ages of 1800–2000 Ma and Palaeoproterozoic ages were obtained from xenocrystic zircons of sillimanite gneiss occurring as rafts in the granites (Pease *et al*. 2001; Vernikovskaya *et al*. 2001).

Thus the lithology and age patterns of the Central Taimyr Belt (Table 4) show important similarities to those of the Seve–Kalak Superterrane in Scandinavia as regards (1) emplacement of gabbros at 700–750 Ma and (2) generation of post-Grenvillian S-type granites from continental crust with Mesoproterozoic and Palaeoproterozoic components. Grenvillian ages corresponding to the 923 and 940 Ma ages reported from Central Taimyr (Table 4) have been recorded from basement plinths of the Baltoscandian rift basins preserved in the Seve Nappe Complex. Thus a rhyolitic lava of the wall-rock of a rift dolerite has yielded a 945 ± 31 Ma age (MSWD 0.93; U–Pb zircon ion microprobe age; Albrecht 2000).

Magmatism during attempted break-up of Rodinia

In the Seve Nappe Complex, formation of the Vistas Granite at 845 ± 14 Ma was intimately related to the emplacement of a gabbroic complex. In the related Kalak Nappe Complex, emplacement of tholeiitic gabbro into the sedimentary Sørøy Succession at 829 ± 18 Ma (Krogh & Elvevold 1990) was the likely reason for generation of granitic dykes. A similar generation of the 873 ± 7 Ma anatectic granites in Scotland was proposed by Millar (1999) based on the identical age (873 ± 6 Ma) of gabbros emplaced into the Moine Supergroup. Ryan & Soper (2001) presented numerical models for generation of granitic melts by mafic dykes intruding the basement beneath the Moine rift basins.

In recent palaeomagnetically derived reconstructions of the North Atlantic tract (Torsvik *et al*. 1996; Dalziel 1997; Weil *et al*. 1998), a network of rift arms separate Laurentia, Siberia and Baltica (Fig. 8). If valid, the correlation of the 830–880 Ma magmatism in Scandinavia, Scotland and Taimyr proposed here can be used to model the break-up of Rodinia. During attempted break-up, mafic intrusions were emplaced along failed arms, generating melting of continental crust and S-type granite formation. These failed arms later developed into successful rifts, in the Sørøy–Seiland complex with emplacement of gabbros at *c*. 700 Ma and gabbros, ultramafic rocks and mafic dyke swarms at 600–550 Ma. In the Baltoscandian rift basins now preserved in the Seve–Kalak Superterrane, mafic dyke swarms of E-MORB affinity and extending for at least 900 km intruded at *c*. 600 Ma

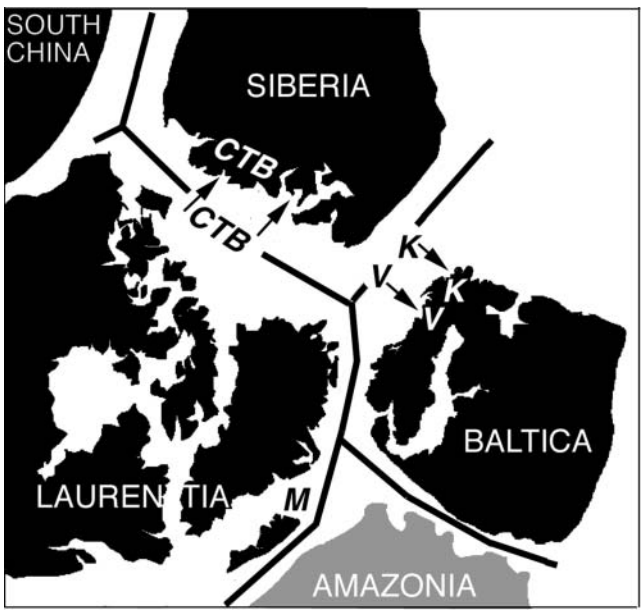

Fig. 8. Reconstruction of Rodinia before break-up at *c*. 600 Ma, showing locations of the *c*. 830–890 Ma magmatism possibly related to abortive break-up. M, Moine; V, Vistas; K, Kalak; CTB, Central Taimyr Belt. Approximate trends of rift arms during successful break-up at *c*. 600 Ma are shown as bold lines. Palaeogeography from Torsvik *et al*. (1996), Dalziel (1997) and Li *et al*. (1999).

(616 Ma at Egersund; 608 Ma in the Sarek Mts). The Seve–Kalak Superterrane accreted to Baltica during the Caledonian Orogeny. The Central Taimyr Complex developed in a region with magmatism of the same tectonic setting and partly similar age as in Scandinavia and Scotland; however, the complex was transported away from the region and accreted to the Siberian craton before late Vendian time (Fig. 8). The associated ophiolites with plagiogranites dated at 720–740 Ma could represent the early ocean floor of successful break-up.

Dalziel & Soper (2001; see also Soper 1994; Soper & England 1995) interpreted the *c*. 870 Ma magmatic event in the Scottish Highlands as the first phase in a two-stage separation of Laurentia from Rodinia (and Pannotia). In south China, restored between Laurentia, Siberia and Australia (Fig. 8), widespread granite formation accompanied rift-related emplacement of mafic and ultramafic dykes and sills at *c*. 830 Ma (Li *et al*. 1999). Mafic dyke swarms occurring along the present-day southern margin of the Siberian craton have been interpreted as related to attempted continental break-up at 855–885 Ma (Sklyarov *et al*. 2001).

This study was financed by a grant from the Swedish Natural Science Research Council to P.G.A. (G 5103-672/1999). The NORDSIM facility is supported by the reseach funding agencies of Denmark, Finland, Norway and Sweden, together with the Swedish Museum of Natural History; we thank Kerstin Lindén, Torbjörn Surde and Martin Whitehouse for technical support and discussions. We acknowledge with appreciation the access to the LA-ICP-MS equipment of the Earth Sciences Centre, Gothenburg University, and thank D. Cornell and W. Meurer for technical assistance and advice. We acknowledge with great thanks careful and very constructive reviews by B. Bingen and S. Daly. This is NORDSIM Publication 72.

References

Aitcheson, S.J. 1990. Nd isotopic evidence for exotic detritus in the Kalak Nappe Complex, north Norwegian Caledonides. *Journal of the Geological Society, London*, **147**, 923–926.

Albrecht, L. G. 2000. *Early structural and metamorphic evolution of the Scandinavian Caledonides: a study of the eclogite-bearing Seve Nappe Complex at the Arctic Circle, Sweden*. PhD thesis, Lund University.

Andréasson, P.G. 1994. The Baltoscandian Margin in Neoproterozoic–Early Palaeozoic time. Some constraints on terrane derivation and accretion in the Arctic Scandinavian Caledonides. *Tectonophysics*, **231**, 1–32.

Andréasson, P.G., Gee, D.G. & Sukotji, S. 1985. Seve eclogites in the Norrbotten Caledonides. *In:* Gee, D.G. & Sturt, B.A. (eds) *The Caledonide Orogen—Scandinavia and Related Areas*. Wiley, Chichester, 887–902.

Andréasson, P.G., Svenningsen, O.M. & Albrecht, L. 1998. Dawn of Phanerozoic orogeny in the North Atlantic tract; evidence from the Seve–Kalak Superterrane, Scandinavian Caledonides. *GFF*, **120**, 159–172.

Bingen, B., Demaiffe, D. & Van Breemen, O. 1998. The 616 Ma old Egersund basaltic dike swarm, SW Norway, and Late Neoproterozoic opening of the Iapetus Ocean. *Journal of Geology*, **106**, 565–574.

Chappell, B.J. & White, A.J.R. 1992. I- and S-type granites in the Lachlan Fold Belt. *In: The Second HnHon Symposium of the Origin of Granites and Related Rocks*. Geological Society of America, Special Papers, **272**, 1–26.

Daly, J.S., Aitcheson, S.J., Cliff, R.A., Gayer, R.A. & Rice, A.H.N. 1991. Geochronological evidence from discordant plutons for a late Proterozoic orogen in the Caledonides of Finnmark, northern Norway. *Journal of the Geological Society, London*, **148**, 29–40.

Dalziel, I.W.D. 1997. Neoproterozoic–Paleozoic geography and tectonics: review, hypothesis, environmental speculation. *Geological Society of America Bulletin*, **109**, 16–42.

Dalziel, I.W.D. & Soper, N.J. 2001. Neoproterozoic extension on the Scottish Promontory of Laurentia; paleogeographic and tectonic implications. *Journal of Geology*, **109**, 299–317.

De la Roche, H., Leterrier, J., Grandclaude, P. & Marchal, M. 1980. A classification of volcanic and plutonic rocks using R1R2-diagram and major element analyses—its relationships with current nomenclature. *Chemical Geology*, **29**, 183–210.

Evensen, N.M., Hamilton, P.J. & O'Nions, R.K. 1978. Rare-earth abundances in chondritic meteorites. *Geochimica et Cosmochimica Acta*, **42**, 1199–1212.

Friend, C.R.L., Kinny, P.D., Rogers, G., Strachan, R.A. & Paterson, B.A. 1997. U–Pb zircon geochronological evidence for Neoproterozoic events in the Glenfinnian Group (Moine Supergroup): the formation of the Ardgour granite gneiss, north-west Scotland. *Contributions to Mineralogy and Petrology*, **128**, 101–113.

Gee, D.G. 1975. A tectonic model for the central part of the Scandinavian Caledonides. *American Journal of Science*, **275A**, 468–515.

Grenne, T., Ihlen, P.M. & Vokes, F.M. 1999. Scandinavian Caledonide metallogeny in a plate tectonic perspective. *Mineralium Deposita*, **34**, 422–471.

Harley, S. 2001. Zircon chemistry and definition of high-grade events in east Antarctica. *Terra Abstracts*, **11**, 375.

Harlov, D.E. & Wirth, R. 2000. K-feldspar–quartz and K-feldspar–plagioclase phase boundary interactions in garnet–orthopyroxene gneisses from the Val Strona di Omegna, Ivrea–Verbano Zone, northern Italy. *Contributions to Mineralogy and Petrology*, **140**, 128–162.

Krogh, E.J. & Elvevold, S. 1990. A Precambrian age for an early gabbro–monzonitic intrusive on the Øksfjord peninsula, Seiland Igneous Province, northern Norway. *Norsk Geologisk Tidsskrift*, **70**, 267–273.

Kumpulainen, R. & Nystuen, J.P. 1985. Late Proterozoic basin evolution and sedimentation in the westernmost part of Baltoscandia. *In:* Gee, D.G. & Sturt, B.A. (eds) *The Caledonide Orogen—Scandinavia and Related Areas*. Wiley, Chichester, 213–232.

Li, Z.X., Li, X.H., Kinny, P.D. & Wang, J. 1999. The breakup of Rodinia: did it start with a mantle plume beneath South China? *Earth and Planetary Science Letters*, **173**, 171–181.

Ludwig, K.R. 1999. *Using Isoplot/Ex, Version 2.01: a Geochronological Toolkit for Microsoft Excel*. Berkeley Geochronology Center Special Publication, **1a**.

Millar, I.L. 1999. Neoproterozoic extensional basic magmatism associated with the West Highland granite gneiss in the Moine Supergroup of NW Scotland. *Journal of the Geological Society, London*, **156**, 1153–1162.

Noble, S.R., Hyslop, E.K. & Highton, A.J. 1996. High-precision U–Pb monazite geochronology of the *c* 806 Ma Grampian Shear Zone and the implications for the evolution of the Central Highlands of Scotland. *Journal of the Geological Society, London*, **153**, 511–514.

Pease, V., Gee, D.G., Vernikovsky, V., Vernikovskaya, A.E. & Kireev, S. 2001. Geochronological evidence for late-Grenvillian magmatic and metamorphic events in central Taimyr, northern Siberia. *Terra Nova*, **13**, 270–280.

Pearce, J.A., Harris, N.B.W. & Tindle, A.G. 1984. Trace element discrimination diagrams for the tectonic interpretation of granitic rocks. *Journal of Petrology*, **25**, 956–983.

Pearce, N.J., Perkins, W.T., Westgate, J.A., Gorton, M.P., Jackson, S.E., Neal, C.R. & Chenery, S.P. 1997. A compilation of new and published major and trace element data for NIST SRM 610 and SRM 612 partially certified glass reference materials. *Geostandards Newsletter*, **21**, 115–144.

Pedersen, R.B., Dunning, G.R. & Robins, B. 1989. U–Pb ages of nepheline syenite pegmatites from the Seiland Magmatic Province, N. Norway. *In:* Gayer, R.A. (ed.) *The Caledonide Geology of Scandinavia*. Graham & Trotman, London, 3–8.

Ramsay, D.M., Sturt, B.A., Zwaan, K.B. & Roberts, D. 1985. Caledonides of northern Norway. *In:* Gee, D.G. & Sturt, B.A. (eds) *The Caledonide Orogen—Scandinavia and Related Areas*. Wiley, Chichester, 163–184.

Reginiussen, H., Krogh Ravna, E.J. & Berglund, K. 1995. Mafic dykes from Øksfjord, Seiland Igneous Province, northern Norway: geochemistry and palaeotectonic significance. *Geological Magazine*, **132**, 667–681.

Rice, A.H.N., Townsend, C. & Robins, B. 1991. *Field Guide to the Caledonides of Finnmark, North Norway*. IGCP 233 Terranes in the Arctic Caledonides, 1–109.

Roberts, D. 1973. *Geologisk kart over Norge, berggrunnskart, Hammerfest 1:250 000*. Norges Geologiske Undersøkelse, Trondheim.

Robins, B. & Gardner, P.M. 1975. The magmatic evolution of the Seiland Province, and Caledonian plate boundaries in northern Norway. *Earth and Planetary Science Letters*, **26**, 167–178.

Rogers, G., Hyslop, E.K., Strachan, R.A., Paterson, B.A. & Holdsworth, R.E. 1998. The structural setting and U–Pb geochronology of Knoydartian pegmatites in W Inverness-shire: evidence for Neoproterozoic tectonothermal events in the Moine of NW Scotland. *Journal of the Geological Society, London*, **155**, 685–696.

Ryan, P.D. & Soper, N.J. 2001. Modelling anatexis in intracratonic basins: an example from the Neoproterozoic rocks of the Scottish Highlands. *Geological Magazine*, **138**, 577–588.

Sandelin, S. 1997. *Tektonostratigrafi och protoliter i Mårma-Vistasområdet, Kebnekaise, Skandinaviska Kaledoniderna*. MSc thesis, Lund University [in Swedish].

Sklyarov, E.V., Gladkochub, D.P., Mazukabzov, A.M., Donskaya, T.V. & Konstantinov, K.M. 2001. Dyke swarms of the marginal part of Siberian craton. *In:* Sklyarov, E.V. (ed.) *Assembly and Breakup of Rodinia Super-*

continent: Evidence From South Siberia. Workshop IGCP-440, Irkutsk, 21–51.

Solyom, Z., Andréasson, P.G. & Johansson, I. 1984. Petrochemistry of Late Proterozoic rift volcanism in Scandinavia II: The Särv Dolerites (SD)—volcanism in the constructive arm of Iapetus. *Lund Publications in Geology*, **35**, 1–42.

Solyom, Z., Lindqvist, J.-E. & Johansson, I. 1992. The geochemistry, genesis, and geotectonic setting of Proterozoic dyke swarms in southern and central Sweden. *Geologiska Föreningens i Stockholm Förhandlingar*, **114**, 47–65.

Soper, N.J. 1994. Was Scotland a Vendian RRR junction? *Journal of the Geological Society, London*, **151**, 579–582.

Soper, N.J. & England, R.W. 1995. Vendian and Riphean rifting in NW Scotland. *Journal of the Geological Society, London*, **152**, 11–14.

Stacey, J.S. & Kramers, J.D. 1975. Approximation of terrestrial lead isotope evolution by a two-stage model. *Earth and Planetary Science Letters*, **26**, 207–221.

Stølen, L.-K. 1996. Caledonian geology of the Pältsa area, northernmost Swedish Caledonides: the termination of the Seve Nappe Complex? *GFF*, **118**, 40–41.

Sturt, B.A. & Taylor, J. 1971. The Timing and Environment of Emplacement of the Storelv Gabbro, Sørøy. *Norges Geologiske Undersøkelse Bulletin*, **272**, 1–34.

Svenningsen, O.M. 2001. Onset of seafloor spreading in the Iapetus Ocean at 608 Ma: precise age of the Sarek dyke swarm, northern Swedish Caledonides. *Precambrian Research*, **110**, 241–254.

Torsvik, T.H., Smethurst, M.A., Meert, J.G. & 5 others 1996. Continental break-up and collision in the Neoproterozoic and Palaeozoic—a tale of Baltica and Laurentia. *Earth-Science Reviews*, **40**, 229–258.

Vernikovskaya, A.E., Pease, V., Vernikovskiy, V.A., Gee, D.G. & Travin, A.V. 2001. The Mamont–Shrenk Neoproterozoic Granitoids (Central Taimyr): geochemistry, petrology and geodynamics. *Journal of Conference Abstracts*, **6**, 754.

Vernikovskiy, V.A., Vernikovskaya, A.E. & Chernykh, A.I. 1998. Neoproterozoic Taymyr Ophiolitic Belts and opening of the Paleo-Pacific Ocean. *International Geology Review*, **40**, 528–538.

Vernikovsky, V.A. & Vernikovskaya, A.E. 2001. Central Taimyr accretionary belt (Arctic Asia): Meso-Neoproterozoic tectonic evolution and Rodinia breakup. *Precambrian Research*, **110**, 127–141.

Vidal, G. & Moczydlowska, M. 1995. The Neoproterozoic of Baltica—stratigraphy, palaeobiology and general geological evolution. *Precambrian Research*, **73**, 197–216.

Vidal, G. & Nystuen, J.-P. 1990. Micropaleontology, depositional environment and biostratigraphy of the Upper Proterozoic Hedmark Group, southern Norway. *American Journal of Science*, **290**, 170–211.

Weil, A.B., Van Der Voo, R., Mac Niocaill, C. & Meert, J.G. 1998. The Proterozoic supercontinent Rodinia: palaeomagnetically derived reconstructions for 1100 to 800 Ma. *Earth and Planetary Science Letters*, **154**, 13–24.

Whitehouse, M. 2000. Combining in situ zircon REE and U–Th–Pb geochronology: a petrogenetic dating tool. *Journal of Conference Abstracts*, **5**, 1086.

Whitehouse, M.J., Bridgewater, D. & Park, R.G. 1997a. Detrital zircon ages from the Loch Maree Group, Lewisian Complex, NW Scotland: confirmation of a Palaeoproterozoic Laurentia–Fennoscandia connection. *Terra Nova*, **9**, 260–263.

Whitehouse, M.J., Claesson, S., Sunde, T. & Vestin, J. 1997b. Ion-microprobe U–Pb zircon geochronology and correlation of Archaean gneisses from the Lewisian Complex of Gruinard Bay, north-west Scotland. *Geochimica et Cosmochimica Acta*, **61**, 4429–4438.

Whitehouse, M.J., Kamber, B.S. & Moorbath, S. 1999. Age significance of U–Th–Pb zircon data from early Archaean rocks of west Greenland—a reassessment based on combined ion-microprobe and imaging studies. *Chemical Geology*, **160**, 201–224.

Wiedenbeck, M., Allé, P., Corfu, F. & 6 others 1995. Three natural zircon standards for U–Th–Pb, Lu–Hf, trace element and REE analysis. *Geostandards Newsletter*, **19**, 1–23.

Winchester, J.A. 1985. Major low-angle fault displacement measured by matching amphibolite chemistry—an example from Scotland. *Geology*, **13**, 604–606.

Received 27 November 2001; revised typescript accepted 18 May 2002.
Scientific editing by Mike Cosca